



The Comparison of Tunnel Convergence from Numerical Analysis with Monitoring Data Based on Different Constitutive Models in Rock Medium

Chalajour, S.¹* and Hataf, N.²*

¹ Ph.D., Graduate Student, Department of Civil Engineering, Shiraz University, Shiraz, Iran.

² Professor, Department of Civil and Environmental Engineering, Shiraz University, Shiraz, Iran.

© University of Tehran 2022

Received: 21 May 2022;

Revised: 12 Sep. 2022;

Accepted: 22 Oct. 2022

ABSTRACT: Tunnels are used for numerous purposes; therefore, proper evaluation and prediction of tunnel behavior, influenced by the surrounding environment's characteristics, is of great concern for civil engineers. In this regard, two water convey and railway tunnels in rock medium were modelled to investigate the influence of various constitutive models on tunnels' behaviors prediction. The tunnel convergence predicted by each constitutive model was compared with the reported monitoring data. Then, the most appropriate constitutive models for tunnel analysis in each rock category were proposed according to the strength of each category's rocks. The results indicated that the Mohr-Coulomb criteria for very weak rocks, the Generalized Hoek-Brown for weak rocks and the Generalized Hoek-Brown with the residual parameter criteria for modelling medium rocks, had more reliable predictions of tunnel convergence. Also, utilizing shear strength parameters correlated from rock mass specific parameters to analyze tunnels in weak and medium rocks was not satisfactory.

Keywords: 3D Finite-Element Simulation, Constitutive Model, Monitoring Data, Rock Tunnel.

1. Introduction

Tunnels are generally used as underground structures for various purposes, including transportation routes, access paths, water transition ducts, powerhouse caverns, underground constructions, etc. Therefore, a proper evaluation and prediction of their behavior, which is influenced mainly by the materials of the surrounding media, is of great concern. Tunnel support system which is required to provide stability and safety, is also affected by tunnel behavior prediction

(Hajiazizi et al. 2021). Various criteria and constitutive models have been proposed to simulate the ground behavior. Numerous studies have been conducted investigating the influence of different constitutive models on tunnel analysis. Oettl et al. (1998), based on the two-dimensional finite element analysis of the Vienna metro tunnel, investigated the effect of four different constitutive models on predicting settlements and stresses in the tunneling environment as well as forces developed in the support system by considering the

* Corresponding author E-mail: nhataf@shirazu.ac.ir

tunnel's monitoring data. Möller and Vermeer (2008), Rukhaiyar and Samadhiya (2016), Hejazi et al. (2008) investigated the results of two-dimensional finite element analysis using three different constitutive models of a hypothetical tunnel. Alejano and Alonso (2005) inspected the effects of constitutive models, for three rock categories, on the ground surface settlements prediction induced by tunneling. Vakili et al. (2014) studied the impact of different constitutive models on mechanized tunneling, for shallow and deep tunnels, by three-dimensional finite element analysis. In a three-dimensional analysis of the TBM tunnel, Jallow et al. (2019) examined the effect of different constitutive models on soil, adjusting surface settlement values with monitoring results. They also analyzed the effect of different parameters on long-term ground surface settlements. Mousivand and Maleki (2018) investigated the results of constitutive models in two-dimensional analysis by convergence-confinement method for shallow circular tunnels. Fong et al. (2022) investigated the appropriate anisotropic soils constitutive model in tunnel analysis by data matching and numerical simulation. Chen and Lee (2020) surveyed the deformation of tunnels by three-dimensional FEM analysis in horseshoe-shaped tunnels in different geological conditions by considering two Mohr-Coulomb and Hoek-Brown constitutive models and indicated that the magnitude and distribution of tunnel deformations were close by these two models. Further researches for analyzing deformations, induced by tunneling and comparing with data monitoring, have also been reported in the literature (Aksoy and Uyar, 2017; Su et al., 2019; Xing et al., 2018; Zhao et al., 2017; Beyabanaki and Gall, (2017), Sharifzadeh et al. (2012), Jin et al. 2020; Sun et al., 2020; Li et al., 2020; Xue et al., 2021).

Although numerous research has been performed on the effects of constitutive models on tunnel's characteristics, most investigations were carried out in the soil

medium, and there is a lack of studies on rock characteristics. Basically, to obtain stresses and strains, a constitutive model is required to be introduced, and the simulations of rock and soil behaviors by utilizing numerical methods depend on the applied constitutive models.

This paper examines the effects of constitutive models on predicting the deformation and convergence of tunnels in homogeneous rock mediums. Based on the RMR classification system, a series of 3D numerical simulations with seven different constitutive models for three rock categories (very weak, weak and medium) commonly used in tunnel analysis have been conducted. Utilized models were Linear Elastic (LE) and Von Mises (VM) as general models; Mohr-Coulomb (MC), Drucker-Prager (DP) and Strain Softening (SS) as classical soil models; Generalized Hoek-Brown (GHB) and GHB with Residual parameters (GHBR) as special rock models.

In the LE model, the stress is linearly correlated with the strain, represented as Hooke's Law:

$$\sigma = E\varepsilon \quad (1)$$

where E : is the Young's modulus of the material; σ and ε : are the stress and strain, respectively. As seen, the constants of this model are only the Young's modulus and the Poisson's ratio. This model does not define a failure criterion.

In the VM model, the yield occurs when the value of the deviatoric stress reaches a critical value (Davis and Selvadurai, 2005). When this constitutive model is applied to a soil material, the effect of hydrostatic pressure is not considered, and the yield surface is the same for both tension and compression (Davis and Selvadurai, 2005). The von Mises yield condition is written as:

$$q = k \quad (2)$$

where q : is the deviatoric stress and k : is the yield stress of the material.

Mohr-Coulomb model is an elastic-perfectly plastic model and is one of the simplest and most widely models employed in geotechnical analyses. This is due to the few numbers of required model parameters and easy determination of them, despite the good model results. This model uses five parameters to express soil behavior. These include modulus of elasticity, E , and Poisson ratio, ν (both from Hooke's law), angle of internal friction, ϕ , and cohesion, c , (where both express the failure criterion), and the dilation angle, ψ , which is used to determine the plastic volume change due to shear stress (Ng et al., 2015). Mohr-Coulomb failure criterion is written as:

$$\tau = c + \sigma \tan \phi \quad (3)$$

where τ and σ : represent the shearing and normal stress on the physical plane through which material failure occurs, respectively.

Drucker-Prager model is a modified von Mises model, introducing a dependence on the mean stress p :

$$q - \xi p = k \quad (4)$$

Constant parameters ξ and k could be selected such that the model agrees with the Coulomb surface. Similar to the Mohr-Coulomb failure criterion, this model is an elastic-perfectly plastic model, and its parameters are not complex. Unlike the MC model with the hexagonal yield surface on the deviatoric stress plane, the DP model has a circular yield surface (Davis and Selvadurai, 2005).

The SS model consists of a linear part until it reaches the peak shear strength value. After that, the failure occurs, and the shear strength is reduced to the residual shear strength. This model consists of three nonlinear parameters to define strain softening. These include peak cohesion, C_p , residual cohesion, C_r , and softening rate, R (MIDAS Information Technology Co., 2018).

The GHB failure criterion is used to estimate the strength and deformations of

jointed rock masses. In this model, three characteristics of rock mass should be considered: uniaxial compressive strength of intact rock, σ_{ci} , Hoek-Brown constant values (i.e., m_i , m_b and s) and Geological Strength Index, GSI, for rock mass (Yasitli, 2016). The modified Hoek-Brown equation is defined by:

$$\sigma_1 = \sigma_3 + \sigma_{ci} \left(m_b \frac{\sigma_3}{\sigma_{ci}} + s \right)^a \quad (5)$$

$$m_b = m_i \exp \left(\frac{GSI - 100}{28} \right) \quad (6)$$

where σ_1 and σ_3 : are maximum and minimum principal stresses, respectively. The Hoek-Brown parameters can be related to MC constitutive model parameters. More details can be found in Hoek et al. (2002), Eberhardt (2012), Chen and Lee (2019), Hoek and Brown (2019), He et al. (2022).

The GHBR constitutive model is obtained by substituting the GSI_{Peak} to $GSI_{Residual}$ in the Hoek-Brown model. This model behaves similar to the SS model and based on plastic softening behavior of rock, calculates smaller values for residual than the peak values. With respect to GSI, rock masses with $GSI > 75$ have brittle behavior, with $25 < GSI < 75$ have softening behavior, and with $GSI < 25$ exhibit complete plastic behavior (MIDAS Information Technology Co., 2018). More information regarding determining the residual parameters based on Hoek-Brown criteria can be found in the investigations of He et al. (2020).

2. Geology, Location and Monitoring of Babolak Water Convey and Isfahan-Shiraz Railway Tunnels

2.1. Babolak Water Convey Tunnel

A cofferdam was constructed at a 700 m distance upstream of Temer Village (Alborz Province, Iran) on Babolak river to provide the required water for the Alborz storage dam. The cofferdam transmits Babolak river water to Babol river at Alborz main dam upstream by a diversion tunnel. Six boreholes were drilled in marl and

marlstone to investigate the properties of the rock as a part of the site investigation of the tunnel. Also, the overburden of the tunnel at three stations of 0 + 550, 0 + 603 and 0 + 638 m was 70, 85 and 89 m, respectively. Three other boreholes at stations 0 + 717, 0 + 732 and 0 + 848 m are located in sandstone with overburden depths equal to 105, 107 and 120 m, respectively. The excavation of the tunnel was performed by a road header machine (Asadollahpour et al., 2014) with an average excavation rate of 1 m/day. The tunnel's support system was shotcrete, wire mesh, a steel frame with 1 m spacing and rock bolts (Asadollahpour, 2011). Due to the sensitivity of the rock mass, after initial drilling, a 5 cm initial layer of shotcrete was applied in order to prevent the effects of moisture and weathering. Then, the steel frames and wire mesh grid were installed,

and the second layer of shotcrete was applied with the progress of the tunnel face. Figure 1 shows the cross-section of the Babolak water convey tunnel. The joints and materials were characterized along the tunnel rout and the results are presented in Tables 1-3.

Table 4 presents the calculated parameters on station 0 + 603 km of Babolak tunnel route, which consists of marl according to RMR classification.

At station 0 + 603, five convergence pins, according to Figure 2 were installed. One was located at the tunnel crown, which is labelled as C, and four were on the wall, labelled as RC, LC, RL and R1L1 in Figure 2.

Figure 3 shows the monitored convergence data at this station for 290 days after the tunnel construction.

Table 1. Rock density ($\frac{gr}{cm^3}$) of the Babolak tunnel (Asadollahpour, E, 2011)

Specimen type	Condition	Number of experiments	STD	AVE	MAX	MIN
Marl	Dry	5	0.17	1.90	2.14	1.73
	Wet	5	0.12	2.17	2.34	2.08
Sandstone	Dry	7	0.16	2.23	2.43	2.00
	Wet	7	0.10	2.38	2.52	2.24

Table 2. Rock uniaxial compressive strength (σ_{ci}) of Babolak tunnel (Asadollahpour, 2011)

Test condition	Rock mass type	Compressive strength (MPa)	Elasticity module (GPa)
Dry	Marl	7.5-15	0.5-7.29
Dry	Sandstone	-	-

Table 3. Discontinuity conditions and characteristics of the route of Babolak tunnel (Asadollahpour, 2011)

	Dip (Deg.)	Dip direction (Deg.)
Bedding	29	129
Discontinuity 1	26	116
Discontinuity 2	46	160
Discontinuity 3	51	300
Discontinuities endurance		1-3 m
Opening		1-5 mm (shallow parts) 0.1-1 mm (Deep parts)
Fillings		5 mm
Roughness		Smooth
Weathering		Little to average
Water condition in discontinuities		Damp

Table 4. Rock parameters of Babolak tunnel

RMR89	Adjustment of joints orientation	Groundwater table condition	Discontinuity condition	Joints spacing (m)	σ_{ci} (MPa)	RQD
Condition/Value	-	Favorable or very favorable	Wet	According to Table 3	1-3	7.5-15 35
Grade	45-57	0 or -2	10	17-12	20-15	2 8

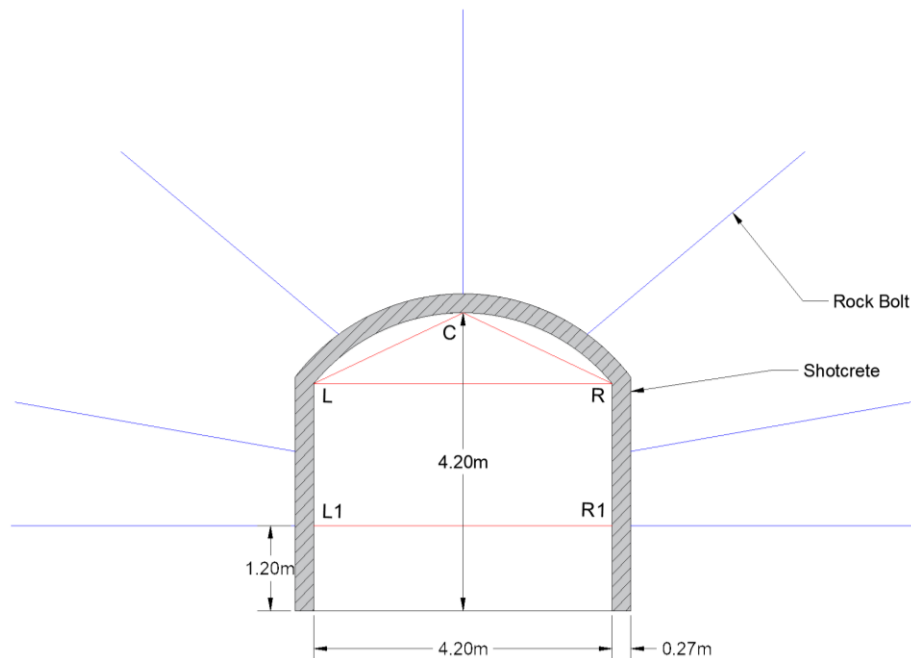


Fig. 1. The cross section of Babolak Tunnel (Dadashi et al., 2012)

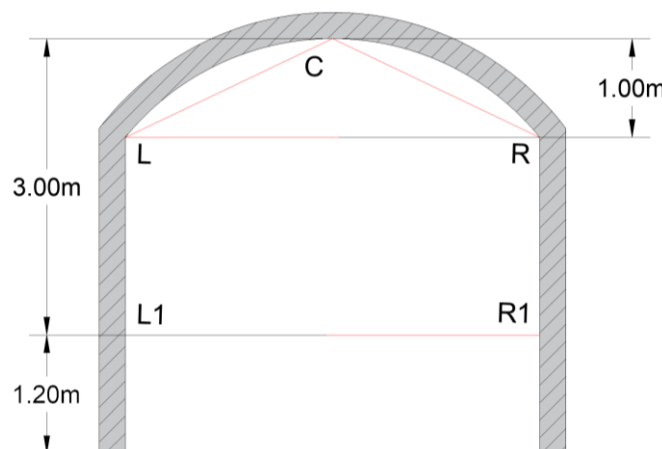
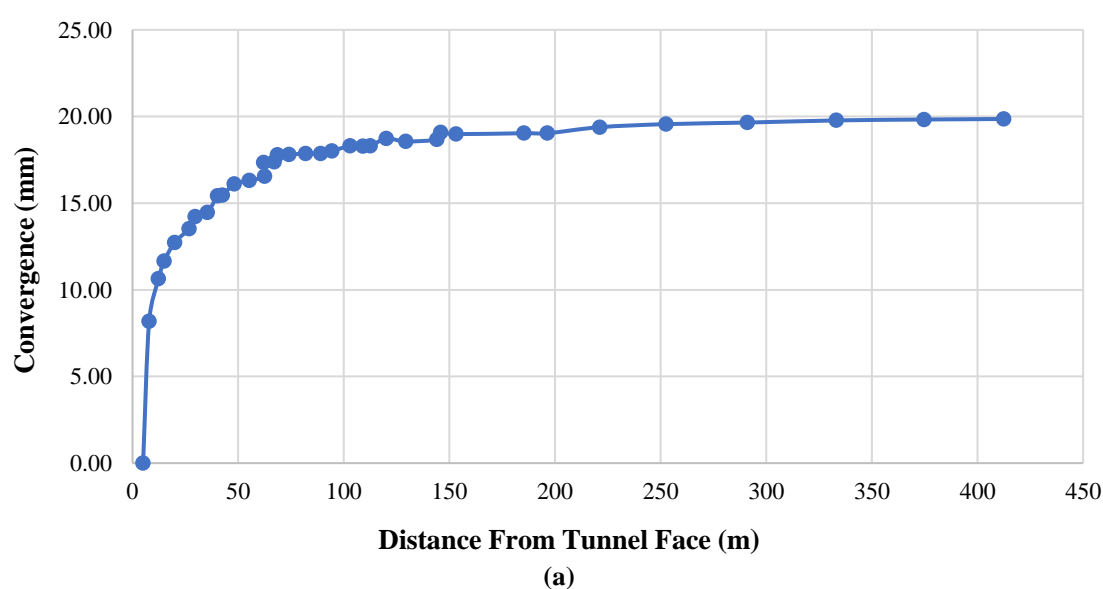


Fig. 2. The position of the monitoring instruments of Babolak tunnel (Asadollahpour, 2011)



(a)

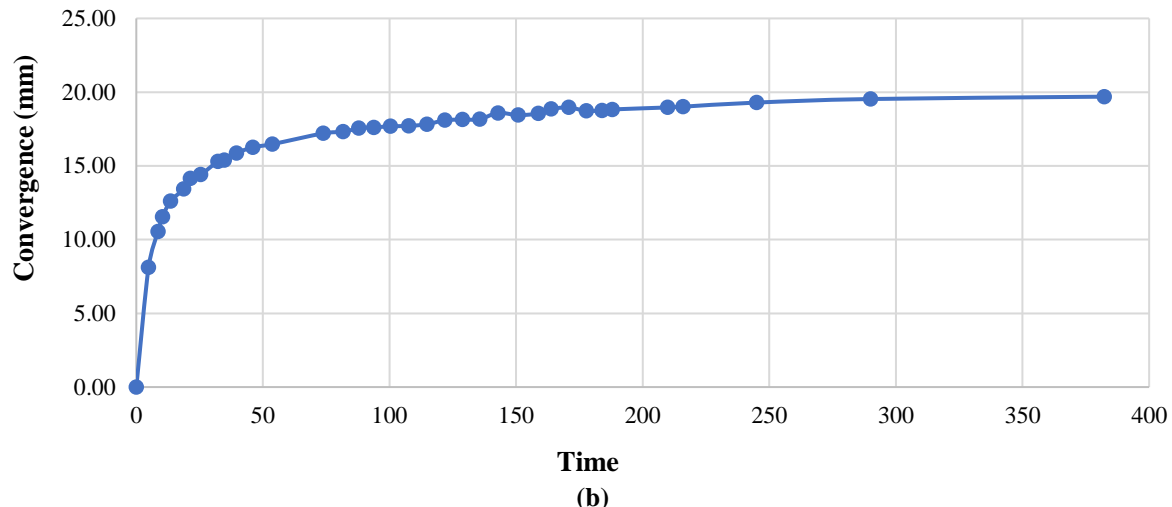


Fig. 3. Convergence data for R1L1 direction: a) According to the distance from the tunnel face; and b) Time at station 0 + 603 (Asadollahpour, 2011)

As shown in Figure 2, the convergence measurements are in the directions of RC, LC, RL, R1L1. The comparison of numerical results has been performed with R1L1 direction results only since due to the presence of the road header, and relatively low convergence in the directions of RC, LC, RL, inaccurate recordings of monitoring data was done. Consequently, the initial measurements of monitoring data were performed at far distances from the tunnel face except for the R1L1 direction, where the first measurements were done at a distance of approximately 3 to 5 m far from the tunnel face (Asadollahpour, 2011).

2.2. Isfahan-Shiraz Railway Tunnel

The Isfahan-Shiraz railway tunnel is located in Fars province (south of Iran). This tunnel is in the Shemshak formation, which is geologically related to the Jurassic

age and includes shale coal and sandstone seams with a horseshoe-shaped cross-section. The tunnel has a length of approximately 820 m and 5.75 m height and 8.2 m in width. Figure 4 illustrates the cross-section of the Isfahan-Shiraz railway tunnel. As shown in this figure, the temporary support system of the tunnel consists of two layers of wire mesh, 25 cm thick shotcrete and the steel frame (Sarikhani Khorami, 2012). The B1-1 convergence station was situated at 269 + 047.5, which is located at a distance of about 717.5 m from the entrance of the tunnel. The tunnel overburden at this station is 29 m high, and the rocks are mostly shale and sandstone. Figure 5 shows the graphs of the tunnel convergence based on the distance from the tunnel axis (Sarikhani Khorami, 2012).

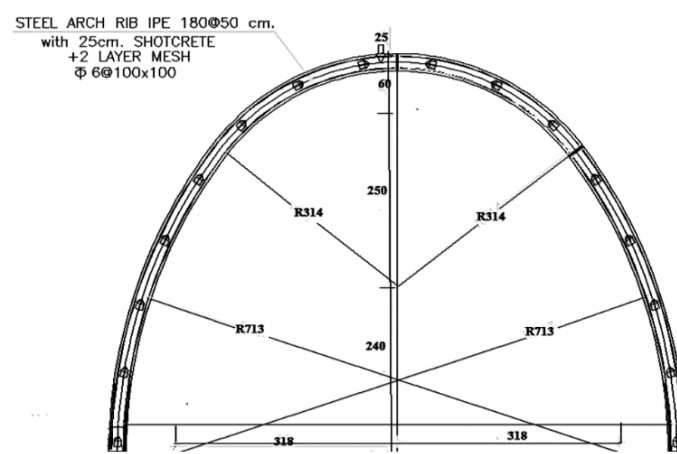


Fig. 4. The cross-section of the Isfahan-Shiraz railway tunnel (Sarikhani Khorami, 2012)

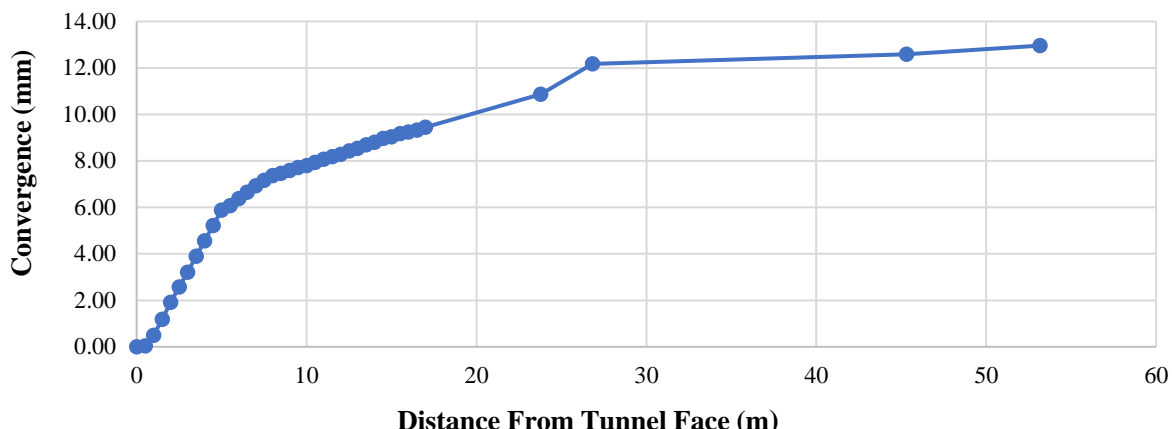


Fig. 5. The tunnel convergence, based on distance from the tunnel face (Sarikhani Khorami, 2012)

3. Determination of Rock Mass Parameters

The rock mass parameters were calculated utilizing RocData software (User's Guide of RocData, 2004) based on the Hoek-Brown failure criterion. The input parameters include compressive strength of intact rock, Geological Resistance Index (GSI), m_i for intact rock, disturbance factor (D), specific gravity of rock and the tunnel depth. Singh and Goel (1999) proposed a relation based on stress measurement in hydraulic fracture test in Himalaya weak rocks for overburden less than 400 m as follows:

$$\sigma_H = 1.5 + 1.2 \sigma_v \quad (7)$$

$$\sigma_h = 1 + 0.5 \sigma_v \quad (8)$$

$$\sigma_v = \gamma \cdot Z \quad (8)$$

where γ : is the unit weight of rock, Z : is the tunnel overburden. The σ_H , σ_h and σ_v : are maximum and minimum horizontal and vertical stresses, respectively. In this study, the mentioned method to determine the horizontal stress was considered.

3.1. Rock Mass Parameters of Babolak Water Convey Tunnel

To determine the rock mass parameters at station 0 + 603 km with an overburden of 88 m, the ratio of in situ horizontal stress coefficient (K) in Babolak water convey tunnel was calculated as 1.5 (Singh and Goel, 1999). According to the mentioned characteristics of the tunnel environment,

the rock mass can be considered as weak to medium rock based on the geomechanics classification or the rock mass rating (RMR) (Bieniawski, 1993). In order to assess according to the RMR system, a site is divided into a number of geological structural units. Then each type of rock mass of the research site is represented by a separate geological structural unit. The six parameters are calculated for each structural unit, including uniaxial compressive strength of intact rock material, Rock Quality Designation (RQD), joint or discontinuity spacing, joint condition, groundwater condition, and joint orientation. Therefore, the RMR classification is determined based on an algebraic sum of ratings for all the parameters mentioned (Goel and Singh, 2011). For this study, the required rock mass information was obtained according to the site investigation and can be found in Tables 1-4. Various research has been conducted to calculate other parameters based on RMR classification.

Moreover, the unit weight and Poisson's ratio were estimated to be 19 kN/m³ and 0.35, respectively, for the weak rock and 20 kN/m³ and 0.3 for the medium rock. Also, the ground disturbance factor (D) was considered as zero for all simulations to reduce influenced factors and consistency for all rock conditions. The disturbance factor greater than zero can influence the behavior of each rock strength category variously. The rest of the calculated values are presented in Tables 5 and 6.

Table 5. The calculated parameters of the Babolak water convey tunnel

Rock type	Sample	σ_{ci}	RMR	GSI	Mi	Em	σ_{cm}	φ	C	ψ	GSI residual	C residual
Unit	-	MPa	-	-	-	MPa	kPa	Deg.	kPa	Deg.	-	kPa
Weak	Marl, Sandy Marl	15	45	40	9	2170	1980	26.71	459	1.9	23.4	327
Medium	Marl, Sandy Marl	15	57	52	9	4350	2600	30.21	560	4.07	25.91	348

Table 6. The Hoek and Brown parameters obtained from RocData for Babolak water convey tunnel

Parameter	a	s	m _b
For weak category	0.511	0.0013	1.056
For medium category	0.505	0.0048	1.621

In Table 5, σ_{ci} : is the uniaxial compressive strength of the intact rock, RMR: is rock mass rating, GSI: is the geological strength index of the rock mass, Mi: is the value of the Hoek-Brown constant, Em: is elastic modulus of the rock mass, σ_{cm} : is the compressive strength of rock mass, φ : is friction angle, C: is cohesion value, ψ : is rock mass dilation angle, GSI and $C_{residual}$: are the residual geological strength index and cohesion of the rock mass, respectively.

3.2. Rock Mass Parameters for Isfahan-Shiraz Railway Tunnel

Table 7 indicates the rock mass parameters of the tunnel environment in addition to the shear strength parameters calculated based on the ground characteristics. According to the characteristics of the tunnel, the site rock mass is located at very weak rock category based on the RMR classification, which could almost be classed as engineering soils (Hoek and Brown, 1997). The behavior of these types of rock mass differs considerably from the tightly interlocked hard rock mass (Hoek et al., 1992). Also, the in-situ horizontal stress in the Isfahan-Shiraz railway tunnel with 29 m overburden

was obtained 2.48. In this table, γ : is rock mass unit weight, κ : is the ratio of horizontal over vertical stress at tunnel depth, and v is Poisson's ratio.

Table 8 summarizes the parameters selected for each constitutive model according to the previous discussion based on the input required parameters in the software. It should be noted that the selected values are based on the median of rock properties categories according to the RMR classification.

4. Numerical Simulation

In this study, the numerical analyses were performed by the commercially available software MIDAS GTS NX 2018; a simulation program developed to evaluate geotechnical aspects and the interaction of soils and structures based on the Finite Element Method (FEM). Moreover, to simulate the longitudinal dimension of the tunnel, Panet equation (Sulem et al., 1987) was used. According to this equation, 98% of the total tunnel displacements occur at a distance of up to 2 times the tunnel diameter from its face. The creep and time-dependent behavior of rocks showed no significant impact at this distance (Asadollahpour et al., 2014).

Table 7. The Ground parameters for the Isfahan-Shiraz railway tunnel

Rock type	Sample	σ_{ci}	RMR	GSI	Mi	Em	σ_{cm}	φ	C	ψ	γ	κ	v
Unit	-	MPa	-	-	-	MPa	kPa	Deg.	kPa	Deg.	kN/m ³	-	-
Very weak	Shale	8.2	17	12	7	321	391	16.15	112	0	24	2.48	0.25

Table 8. Input parameters for each constitutive model for numerical simulations

Rock type	Constitutive model	E_m (MPa)	γ (kN/m ³)	v	σ_{cm} (kPa)	Φ (Deg.)	C (kPa)	Ψ (Deg.)	$C_{residual}$ (kPa)	a	s	m_b	GSI	GSI residual
Very weak	EL	321	24	0.2 5	-	-	-	-	-	-	-	-	-	-
	VM	321	24	0.2 5	391	-	-	-	-	-	-	-	-	-
	DP	321	24	0.2 5	-	16.1 5	11 2	0	-	-	-	-	-	-
	MC	321	24	0.2 5	-	16.1 5	11 2	0	-	-	-	-	-	-
Weak	EL	217 0	19	0.3 5	-	-	-	-	-	-	-	-	-	-
	VM	217 0	19	0.3 5	198 0	-	-	-	-	-	-	-	-	-
	DP	217 0	19	0.3 5	-	26.7 1	45 9	1.9	-	-	-	-	-	-
	MC	217 0	19	0.3 5	-	26.7 1	45 9	1.9	-	-	-	-	-	-
	SS	217 0	19	0.3 5	-	26.7 1	45 9	1.9	32 7	-	-	-	-	-
	GHB	217 0	19	0.3 5	-	-	-	-	-	0.51 1	0.001 3	1.05 6	40	-
	GHB R	217 0	19	0.3 5	-	-	-	-	-	0.51 1	0.001 3	1.05 6	40	23.4
	EL	435 0	20	0.3	-	-	-	-	-	-	-	-	-	-
Medium	VM	435 0	20	0.3	260 0	-	-	-	-	-	-	-	-	-
	DP	435 0	20	0.3	-	30.2 1	56 0	4.0 7	-	-	-	-	-	-
	MC	435 0	20	0.3	-	30.2 1	56 0	4.0 7	-	-	-	-	-	-
	SS	435 0	20	0.3	-	30.2 1	56 0	4.0 7	34 8	-	-	-	-	-
	GHB	435 0	20	0.3	-	-	-	-	-	0.50 5	0.004 8	1.62 1	52	-
	GHB R	435 0	20	0.3	-	-	-	-	-	0.50 5	0.004 8	1.62 1	52	25.9 1

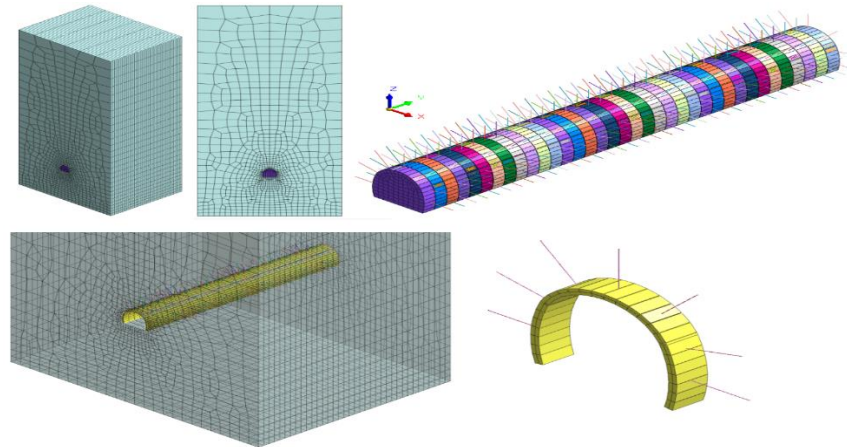
4.1. Numerical Simulation of Babolak Water Convey Tunnel

Dimensions of the FEM model for this tunnel are $46.5 \times 114 \times 36$ m and the numerical modeling results are extracted within 5 m of the tunnel face, corresponding to field measurements. The dimensions of the Finite Element (FE) models are considered to be greater than five times the tunnel diameter on each side (Vitali et al., 2018) and 12 times greater than the tunnel diameter in the longitudinal direction. The tunnel face is located at a distance of 6 times the diameter of the tunnel's beginning.

According to the 4.2 m span of the Babolak water convey tunnel, the results are considered 13 m in the longitudinal direction of numerical modeling compared with monitoring data. Table 9 shows the properties and types of the tunnel support system in the numerical modeling. The equivalent thickness of the shotcrete and steel frame was considered 26.6 cm in numerical simulation, and 25 mm diameter rebars of AIII steel were utilized for rock bolts. Figure 6 shows the FE model of the tunnel in the software.

Table 9. Properties of Babolak water convey tunnel support system in numerical modeling

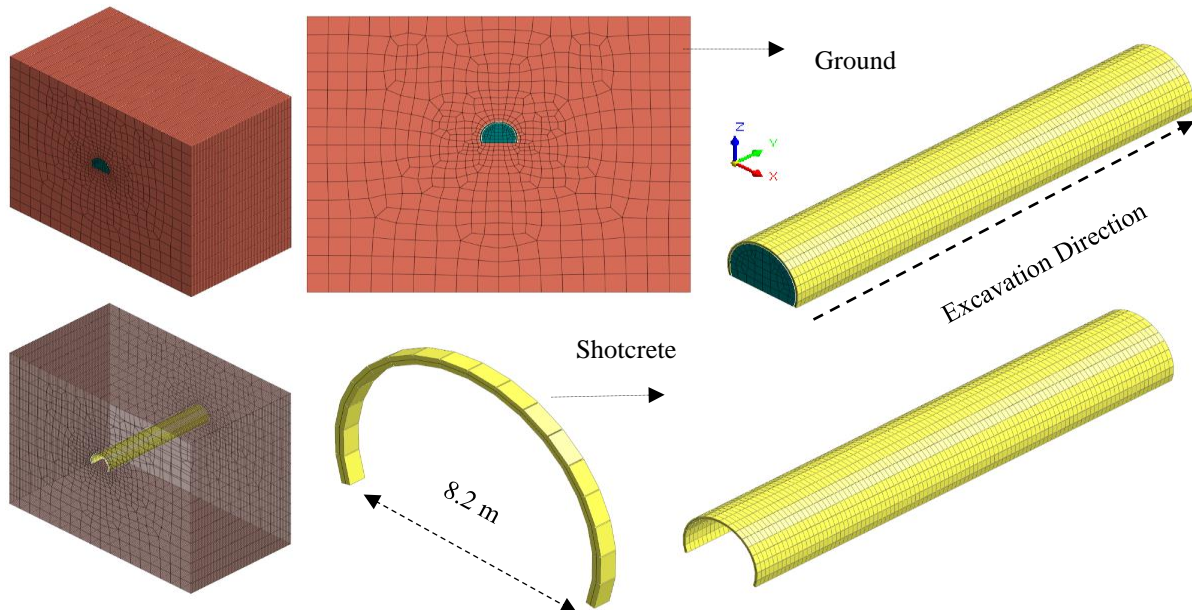
Parameter	Rock bolt	Shotcrete and Latice
Material	Steel	Concrete
Model type	Elastic	Elastic
Mesh type	1D-EMBEDDED truss	2D-shell
Elastic modulus(kPa)	2.1×10^8	2.2×10^7
Thickness	2.5	26.6
Poisson's ratio	0.3	0.25
Density (kN/m ³)	78	24

**Fig. 6.** Babolak tunnel cross-section and support system FE models

4.2. Numerical Simulation of Isfahan-Shiraz Railway Tunnel

Seventeen meters of the Isfahan-Shiraz railway tunnel with 8.2 m span was considered for numerical modeling. The simulation steps were whole cross-section drilling and applying shotcrete simultaneously. The average distance between the tunnel face and the installation of the support system is approximately 0.5

m, and the temporary tunnel support system was modeled as the equivalent of shotcrete thickness. Figure 7 shows the FE model of the tunnel. Shotcrete material properties are also mentioned in Table 8. The boundary conditions of the models were applied by closing the degrees of freedom in the vertical direction and vertical and horizontal directions at the side and bottom of the model, respectively.

**Fig. 7.** Isfahan-Shiraz railway tunnel cross section and support system models in software

The numerical modeling procedure for both tunnels was conducted in seven steps:

- 1- Define the model geometry;
- 2- Define the material constitutive model and support system material parameters;
- 3- Excavation and support system in the geometry of the model;
- 4- Define boundary conditions and mesh generation;
- 5- Define analysis sequence in the mesh of the model (Stage construction sequence: Apply the in-situ condition, Ground excavation, Application and activation of the tunnel support systems);
- 6- Perform analysis;
- 7- Compare the obtained results with monitoring data.

5. Results and Discussions

The results of the numerical analysis of the Isfahan-Shiraz tunnel as well as the Babolak water convey tunnel were compared with the monitoring data of each tunnel.

5.1. Very Weak Rocks (Isfahan-Shiraz Railway Tunnel)

In this rock category, rock-specific constitutive models (GHB and GHBR) and SS were not able to converge equilibrium equations, and only simulation with four constitutive models of LE, VM, DP, and MC indicated the results. It is believed that the very weak rocks behave as a geomaterial; therefore, the rock-specific models are not able to analyze the geomaterial properties. Investigations have revealed that the relationship between RMR and m and s is no longer linear in these very low ranges; therefore, the rock mass specific model of Hoek-Brown cannot be suitable for this rock category (Hoek et al., 2000).

Input parameters for each model are mentioned in Table 7 and were consistent during the analysis in order to obtain the predicted convergence value for each constitutive behavior model. For instance, elastic modulus and Poisons ratio were considered 321 Mpa and 0.25, respectively,

for this rock category. The shear strength parameters, including cohesion value and friction angle, also were considered 112 kPa and 16.12 degrees. These shear strength parameters were the same for MC and DP models. Moreover, the uniaxial shear strength parameter for the rock mass was derived at 391 kPa based on very weak rock strength properties.

The predicted values of the tunnel convergence under the four mentioned constitutive models and monitoring data are presented in Figure 8. The results of the numerical simulation considered for approximately 16 m in order to reduce the influence of the time-dependent behavior of rock mass in numerical simulation. It can be observed that MC constitutive model can predict the results in good agreement with the monitoring data of the tunnel. The VM model showed higher values of convergence, and both LE and DP models showed lower than the monitoring data.

5.2. Weak Rocks (Babolak Water Convey Tunnel)

Similarly, for all numerical simulations in weak rocks, the input parameters of the selected models were considered constant. The elastic modulus and Poisson's ratio were 2170 Mpa and 0.35, respectively. Also, the shear strength parameters for MC and DP were 459 kPa and 26.51 degrees. Other required parameters as input values for behavior models can be found in Tables 5 and 6.

In this rock category, the equations of all seven constitutive models were converged in numerical modeling. As shown in Figure 9 the GHB model is in good agreement with the monitoring results, but SS and the GHBR models showed the tunnel convergence value greater difference than the monitoring data. In this category, the general (LE and VM) and soil (MC and DP) constitutive models provided approximately similar results, which are less than the values predicted by rock mass constitutive models. The figures from these models are coincident in Figure 9. It can be

justified as the rock mass specific constitutive models consider the rock mass strength properties with parameters such as disturbance factor, uniaxial compressive strength, rock classification coefficient and

geological strength index; therefore, these models have more realistic results compared with general and soil mechanics models for rock mass analysis.

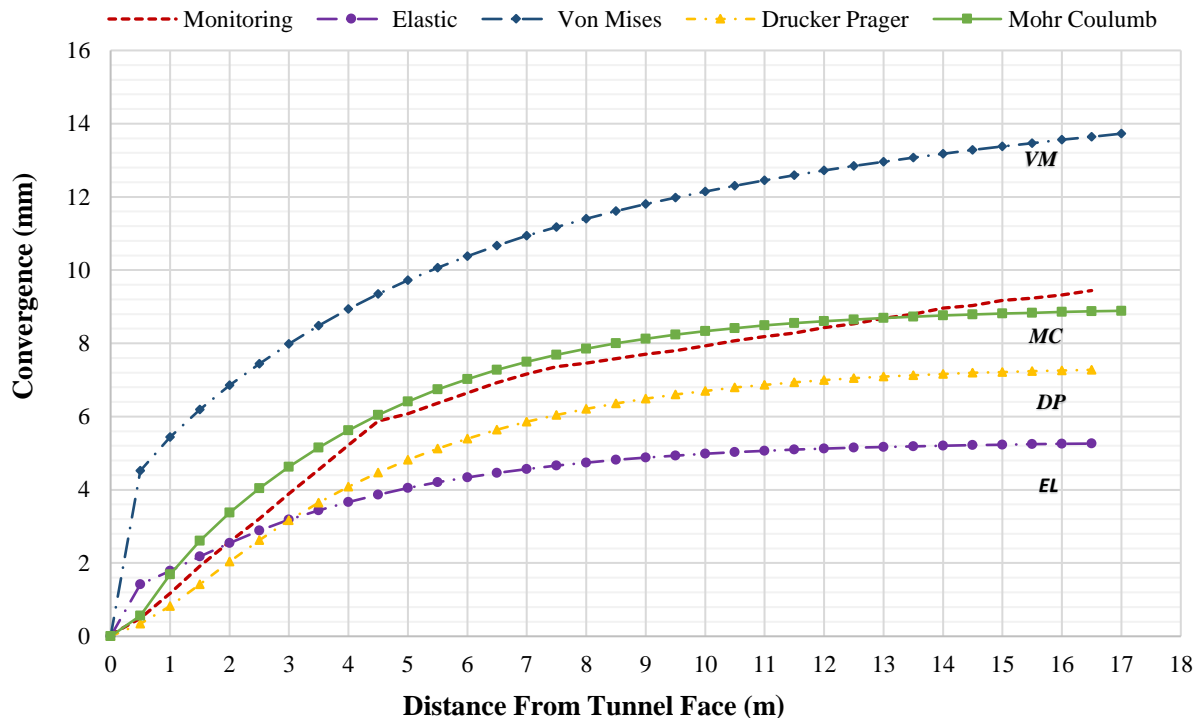


Fig. 8. The comparison of Isfahan-Shiraz railway tunnel modeling results with monitoring data in very weak rock

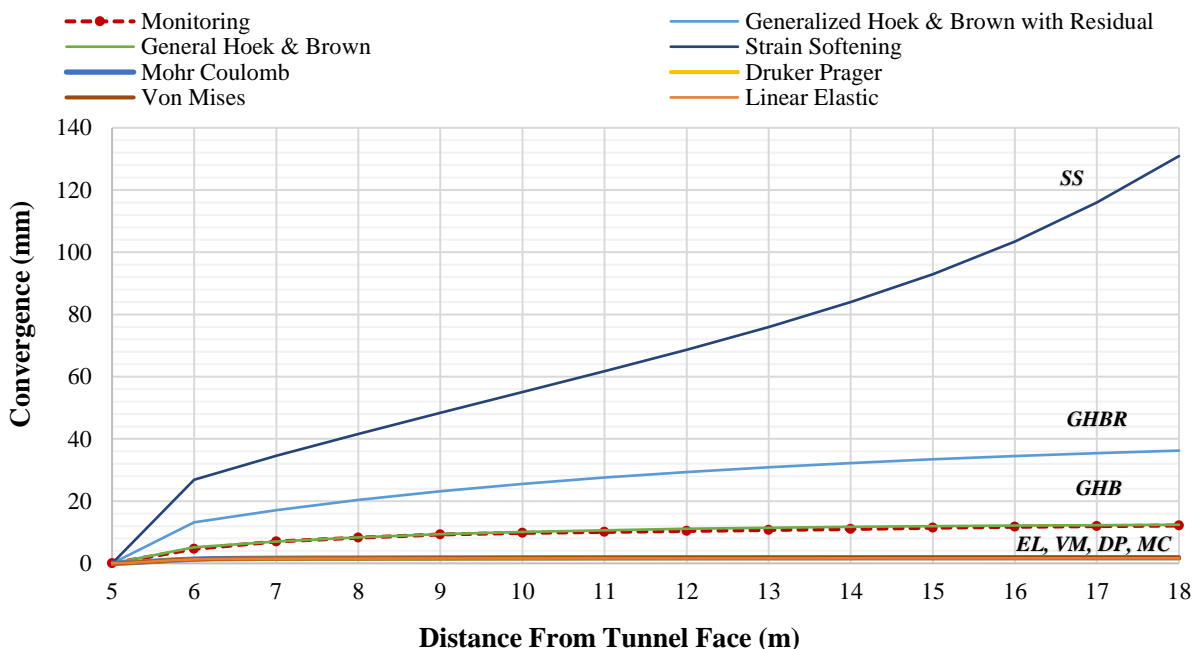


Fig. 9. The Comparison of Babolak Water convey tunnel numerical modeling results with monitoring in weak rock category

5.3. Medium Rocks (Babolak Water Convey Tunnel)

Input parameters for medium rocks were mentioned in Tables 5 and 6. In this category of rocks, the equations of all seven constitutive models were converged in numerical modeling. According to Figure 10, the results of the GHBR were most compatible with the monitoring data, and the LE, VM, DP, as well as MC, showed the same results and were lower than the monitoring data. Therefore, the predicted values are coincident in Figure 10. In this category, the GHB indicated the tunnel convergence of nearly one-quarter, and SS showed almost twice the monitoring data. The other general and soil mechanics models showed the same results and by far less than the monitoring data. However, the GHBR predicted the results in good agreement with the monitoring data.

5.4. Comparison of Numerical Analysis Results of Tunnel Crown Settlement Profile

Figure 11 presents the values of crown settlements along with the longitudinal axis of the mentioned tunnels, obtained from numerical analysis using different constitutive models for the three rock categories of very weak, weak and medium. According to Figure 11 in very weak rock categories (Isfahan-Shiraz railway tunnel), the VM constitutive model predicted the vertical crown settlements at the front of the tunnel face 14.35 mm and more than that of other models. The values of 12.15, 7.58, and 2.44 mm were also obtained for the vertical crown settlements at the tunnel face for MC, DP, and LE constitutive models, respectively. Moreover, the difference between the two models of MC and DP is considerable, and the MC constitutive model showed higher values than the DP

model. The least value was predicted by LE. In the numerical simulation in this rock category, the constitutive models of GHB, GHBR and SS were not converged.

According to Figures 12 and 13, in the weak and medium rock categories (Babolak water convey tunnel), three constitutive models of VM, DP, and MC showed approximately the same values for the vertical settlements of the tunnel crown. Also, the LE model indicated the crown settlement slightly lower values than the models mentioned above. However, SS model in the weak and medium rock categories showed the crown settlement more than all other constitutive models. From the GHB and GHBR models, the crown settlement was higher than the other models. Table 10 summarizes the values of the crown settlement of the tunnel for two categories of weak and medium rocks.

5.5. Investigation of Rocdata and Back Analysis Shear Strength Parameters in Convergence Value

Calculation of shear strength parameters of rock mass in the absence of experimental lab test data was performed by back analysis and empirical equations for this study. As mentioned in Section 4, the shear strength parameters calculated by RocData were derived from the Hoek and Brown parameters. In this section, a comparison of the shear strength data obtained from the back analysis and RocData is performed. Table 11 indicates the difference between the results of back analysis and the obtained shear strength parameters from rock mass parameters. Furthermore, Figure 14 compares the numerical modeling results based on the shear strength parameters obtained from the two mentioned methods with Babolak water convey tunnel monitoring data.

Table 10. The amount of crown settlement in Babolak tunnel face (mm)

	Elastic	Von mises	Drucker prager	Mohr coulomb	Generalized Hoek and Brown	Generalized Hoek and Brown with residual
Weak rocks	0.68	0.72	0.7	0.74	2.78	5.41
Medium rocks	0.42	0.43	0.43	0.43	1.00	2.17

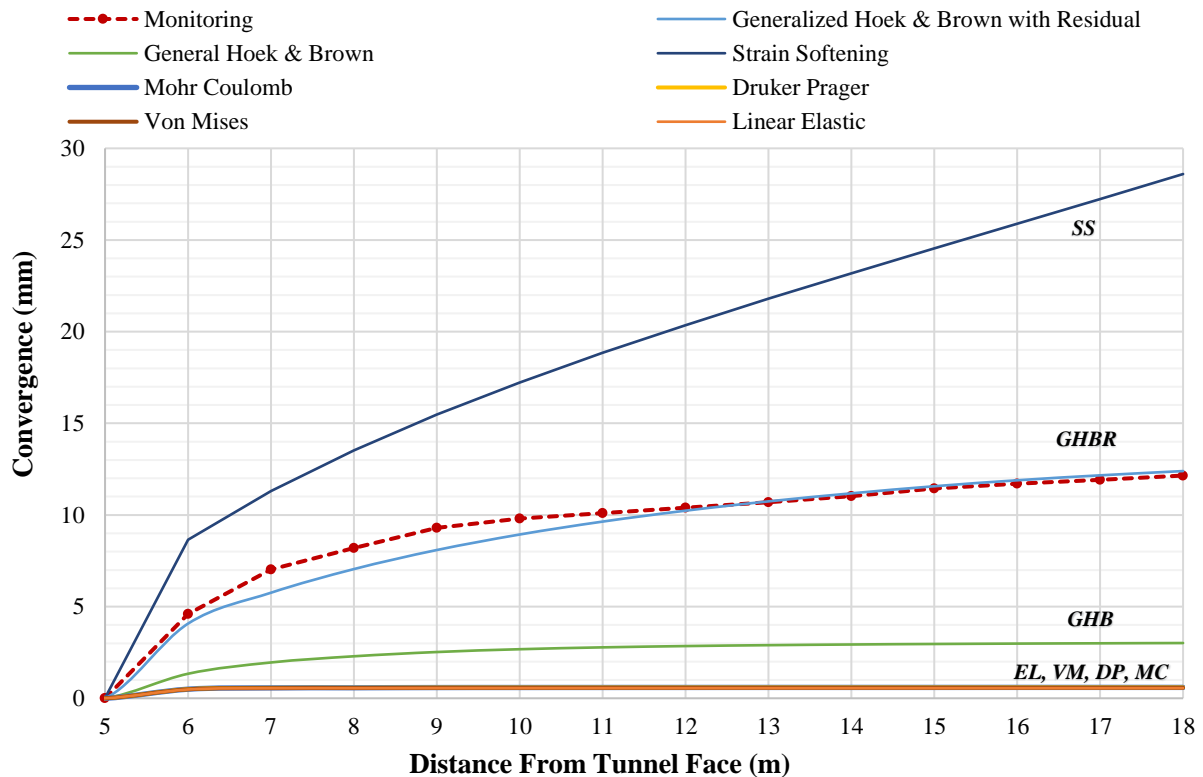


Fig. 10. The Comparison of Babolak water convey tunnel numerical modeling results with monitoring in medium rock category

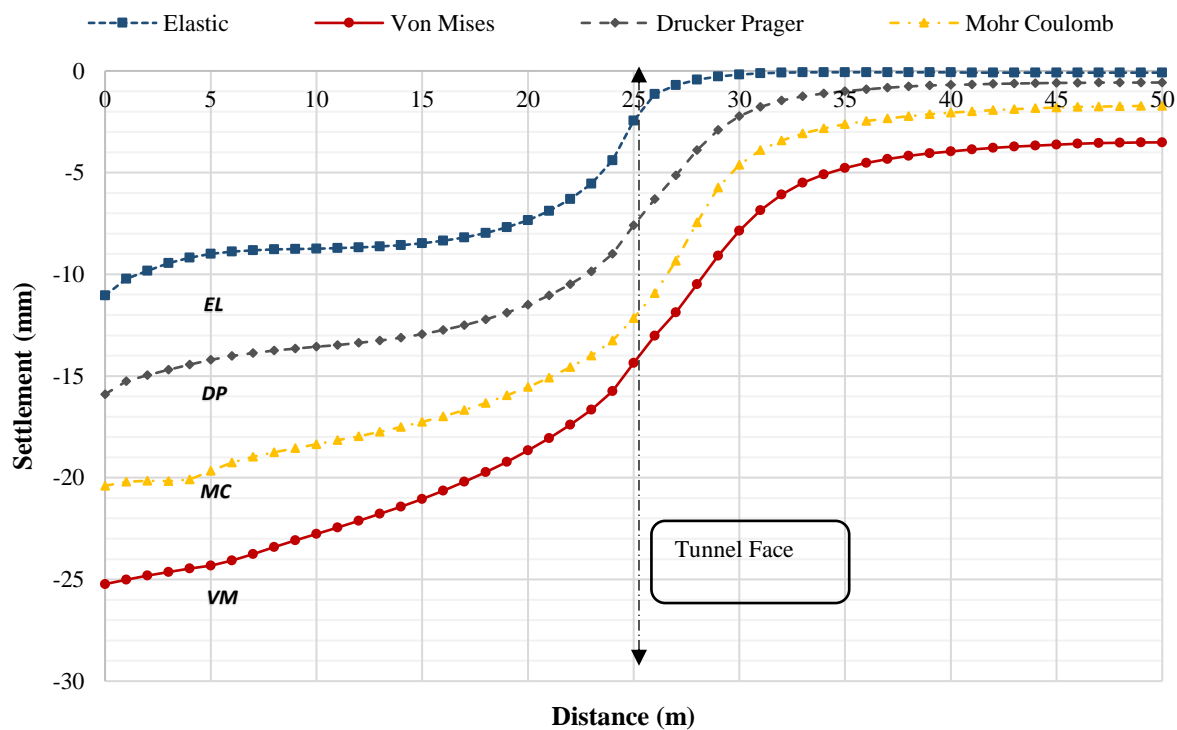


Fig. 11. The Comparison of Babolak water convey tunnel numerical modeling results with monitoring in medium rock category

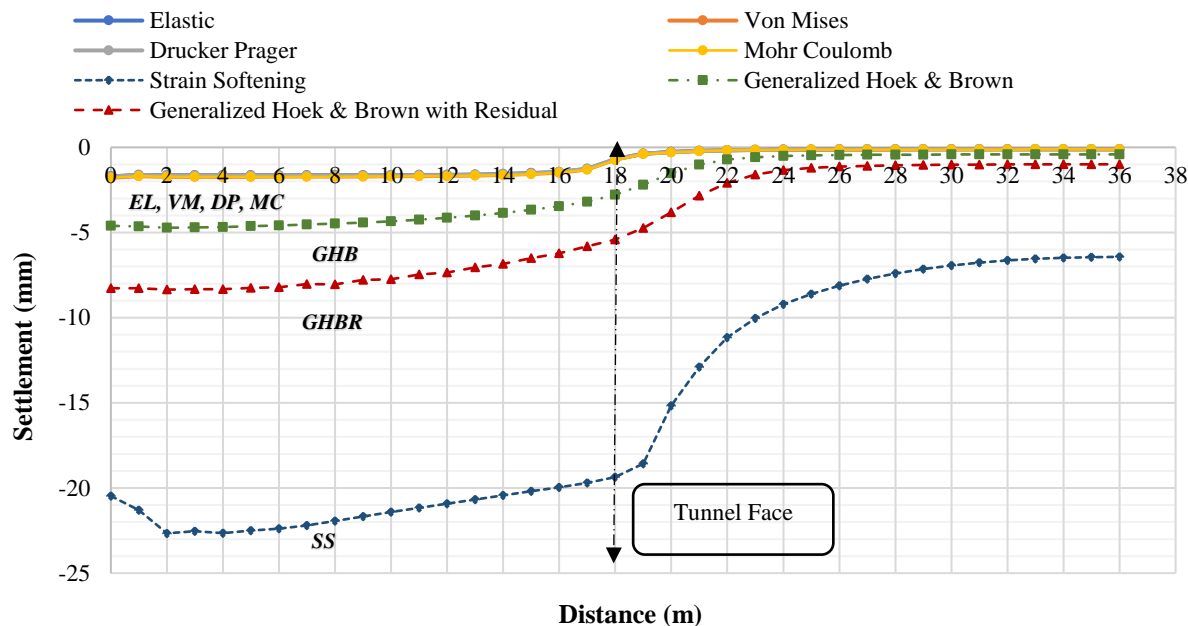


Fig. 12. Crown settlement values along the longitudinal axis of the tunnel obtained from numerical analysis of Babolak water convey tunnel in weak rock category

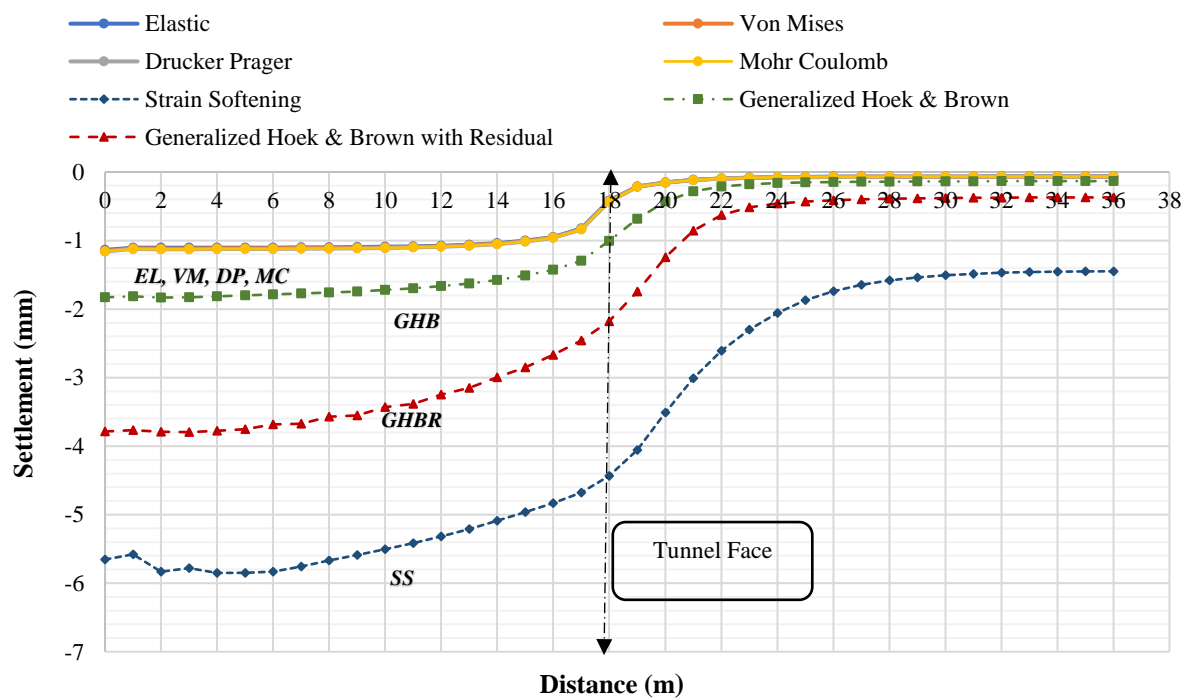


Fig. 13. Crown settlement values along the longitudinal axis of the tunnel obtained from numerical analysis of Babolak water convey tunnel in medium rock category

Table 11. Comparison of the results of shear strength parameters obtained from RocData software and back analysis for Babolak water convey tunnel

Parameter	Cohesion (kPa)	Friction angle (Deg.)	Elastic modules (MPa)
RocData	459	26.7	2170
Back analysis	90	27.0	2170

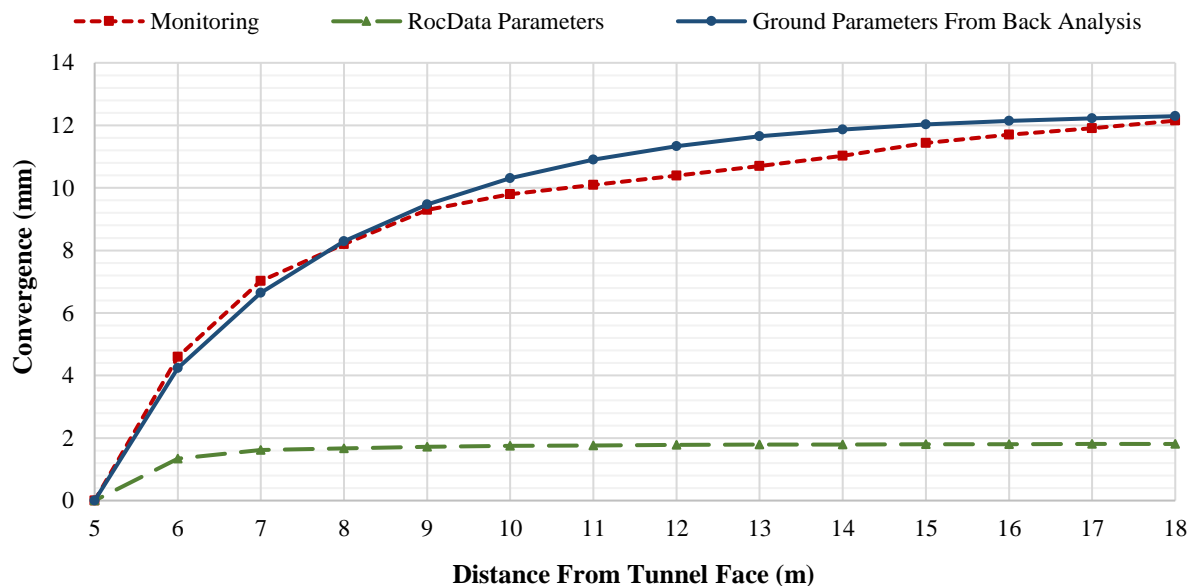


Fig. 14. Comparison of crown settlement values along the longitudinal axis of the tunnel with RocData and back analysis shear strength parameters of Babolak water convey tunnel in medium category of rocks

It can be understood from Table 10 that in the constant elastic modulus, the friction angle of the RocData was pretty close to the friction angle calculated from the back analysis method. However, the obtained cohesion value based on the correlation from the Hoek and Brown theory was approximately five times the cohesion calculated from the back analysis.

6. Conclusions

In this study, tunnel behaviors were examined under different constitutive models in three rock categories. Initially, calculating the rock mass parameters in the absence of sufficient experimental data and in-situ tests was discussed. Then, two case studies of Babolak water convey and Isfahan-Shiraz railway modeled in the finite element software in order to assess the influence of various constitutive models on the tunnels' face convergence and ground settlement. The obtained results from the numerical simulations were compared with the monitoring data to propose the most appropriate model for tunnel analysis in rocks. Then, a comparison was made between the correlation of the shear

parameters from the empirical equations and the back analysis approach. According to the performed analyses, the following results are presented in predicting the behavior of rock tunnels for the assumed conditions in this study:

- Since constitutive models represent the material behavior, they can significantly influence the analysis results. Therefore, utilizing an appropriate constitutive model is the most stage in numerical modeling, and it should be implemented based on accurate data.
- The LE model does not have a failure criterion and utilizing this model should be with caution where there is a probability of failure of the elements.
- The MC model was in the good agreement range with the monitoring data in very weak rocks. However, the difference between the convergence of MC and DP was not significant for this rock category.
- The GHBR showed more convergence values than the monitoring data in the category of weak rocks. According to the recommended range of GSI index for the softening behavior of rocks, weak rocks are placed at the beginning of the

- softening behavior interval; therefore, the results of this model cannot be reliable. However, GHB constitutive model results were almost in accordance with the monitoring data. Thus, the GHB model is suggested in this category of rocks.
- For the medium rocks, as this category is located at the recommended range of softening behavior of rocks, this behavior of the rock mass should be considered in the analysis. Also, the predictions of GHBR model from numerical analysis are almost compatible with monitoring data.
 - Although soil shear strength parameters can be obtained by correlation from the rock mass parameters, the difference between the results of the correlated data and parameters from back analysis was considerable in weak and medium rocks.
 - It is recommended to use rock-specific constitutive models to analyze the tunnels in rock medium since the rock mass conditions are taken into account in these models. However, in very weak rocks that behave similar to soils, shear strength tests may be used to determine the model parameters.

7. References

- Aksoy, C.O. and Uyar, G.G. (2017). "Non-deformable support system in swelling and squeezing rocks", In: *Rock Mechanics and Engineering*, Volume 4 (pp. 179-203), CRC Press.
- Alejano, L.R. and Alonso, E. (2005). "Considerations of the dilatancy angle in rocks and rock masses", *International Journal of Rock Mechanics and Mining Sciences*, 42(4), 481-507, <https://doi.org/10.1016/j.ijrmms.2005.01.003>.
- Asadollahpour, E. (2011). "An investigation into the behaviour of a tunnel in a viscoplastic medium case study: Babolak water conveyance tunnel", M.Sc. Thesis, Shahid Bahonar University of Kerman, Kerman, Iran.
- Asadollahpour, E., Rahmanejad, R., Asghari, A. and Abdollahipour, A. (2014). "Back analysis of closure parameters of Panet equation and Burger's model of Babolak water tunnel conveyance", *International Journal of Rock Mechanics and Mining Sciences*, 68, 159-166, <https://doi.org/10.1016/j.ijrmms.2014.02.017>.
- Beyabanaki, A.R. and Gall, V. (2017). "3D numerical parametric study of the influence of open-pit mining sequence on existing tunnels", *International Journal of Mining Science and Technology*, 27(3), 459-466, <https://doi.org/10.1016/j.ijmst.2017.03.018>.
- Bieniawski, Z.T. (1993). "Classification of rock masses for engineering: The RMR system and future trends", In: *Rock Testing and Site Characterization*, (pp. 553-573), Pergamon, <https://doi.org/10.1016/B978-0-08-042066-0.50028-8>.
- Chen, S.-L. and Lee, S.-C. (2020). "An investigation on tunnel deformation behavior of expressway tunnels", *Geomechanics and Engineering*, 21(2), 215-226, <https://doi.org/10.12989/gae.2020.21.2.215>.
- Chen, Y. and Lin, H. (2019). "Consistency analysis of Hoek–Brown and equivalent Mohr–Coulomb parameters in calculating slope safety factor", *Bulletin of Engineering Geology and the Environment*, 78(6), 4349-4361, <https://doi.org/10.1007/s10064-018-1418-z>.
- Dadashi, E., Ahangari, K., Noorzad, A. and Arab, A. (2012). "Support system suggestion based on back-analysis results case study: Babolak water conveyance tunnel", *Arabian Journal of Geosciences*, 5(6), 1297-1306.
- Davis, R.O. and Selvadurai, A.P.S. (2005). *Plasticity and geomechanics*, Cambridge University Press.
- Eberhardt, E. (2012). "The hoek–brown failure criterion", In: *The ISRM Suggested Methods for Rock Characterization, Testing and Monitoring: 2007-2014*, (pp. 233-240), Springer, Cham.
- Fang, Y., Cui, J., Wanatowski, D., Nikitas, N., Yuan, R. and He, Y. (2022). "Subsurface settlements of shield tunneling predicted by 2D and 3D constitutive models considering non-coaxiality and soil anisotropy: A case study", *Canadian Geotechnical Journal*, 59(3), 424-440, <https://doi.org/10.1139/cgj-2020-062>.
- Goel, R.K. and Singh, B. (2011). *Engineering rock mass classification: Tunnelling, foundations and landslides*, Elsevier.
- Hajizadi, M., Taban, M.H. and Ghobadian, R. (2021). "Prediction of Q-value by multi-variable regression and novel Genetic Algorithm based on the most influential parameters", *Civil Engineering Infrastructures Journal*, 54(2), 267-280, <https://doi.org/10.22059/CEIJ.2020.295339.164>.
- He, M., Zhang, Z., Zhu, J. and Li, N. (2022). "Correlation between the constant mi of Hoek–Brown criterion and porosity of intact rock", *Rock Mechanics and Rock Engineering*, 55(2), 923-936.
- He, M., Zhang, Z., Zheng, J., Chen, F. and Li, N. (2020). "A new perspective on the constant mi of the Hoek–Brown failure criterion and a new

- model for determining the residual strength of rock", *Rock Mechanics and Rock Engineering*, 53(9), 3953-3967, <https://doi.org/10.1007/s00603-020-02164-6>.
- Hejazi, Y., Dias, D. and Kastner, R. (2008). "Impact of constitutive models on the numerical analysis of underground constructions", *Acta Geotechnica*, 3(4), 251-258, <https://doi.org/10.1007/s11440-008-0056-1>.
- Hoek, E., Carranza-Torres, C. and Corkum, B. (2002). "Hoek-Brown failure criterion-2002 edition", *Proceedings of NARMS-Tac*, 1(1), 267-273.
- Hoek, E. and Brown, E.T. (1997). "Practical estimates of rock mass strength", *International Journal of Rock Mechanics and Mining Sciences*, 34(8), 1165-1186, [https://doi.org/10.1016/S1365-1609\(97\)80069-X](https://doi.org/10.1016/S1365-1609(97)80069-X).
- Hoek, E. and Brown, E.T. (2019). The Hoek-Brown failure criterion and GSI-2018 edition", *Journal of Rock Mechanics and Geotechnical Engineering*, 11(3), 445-463, <https://doi.org/10.1016/j.jrmge.2018.08.001>.
- Hoek, E., Kaiser, P.K. and Bawden, W.F. (2000). *Support of underground excavations in hard rock*, CRC Press.
- Hoek, E., Wood, D. and Shah, S. (1992). Support of underground excavations in hard rock, A modified Hoek-Brown failure criterion for jointed rock masses", In: *Rock Characterization: ISRM Symposium, Eurock'92*, Chester, UK, 14-17 September, (pp. 209-214), Thomas Telford Publishing.
- Jallow, A., Ou, C.Y. and Lim, A. (2019). "Three-dimensional numerical study of long-term settlement induced in shield tunneling", *Tunnelling and Underground Space Technology*, 88, 221-236, <https://doi.org/10.1016/j.tust.2019.02.021>.
- Jin, Y.F., Zhu, B.Q., Yin, Z.Y. and Zhang, D.M. (2019). "Three-dimensional numerical analysis of the interaction of two crossing tunnels in soft clay", *Underground Space*, 4(4), 310-327, <https://doi.org/10.1016/j.undsp.2019.04.002>.
- Li, C., Hou, S., Liu, Y., Qin, P., Jin, F. and Yang, Q. (2020). "Analysis on the crown convergence deformation of surrounding rock for double-shield TBM tunnel based on advance borehole monitoring and inversion analysis", *Tunnelling and Underground Space Technology*, 103, 103513, <https://doi.org/10.1016/j.tust.2020.103513>.
- MIDAS Information Technology Co. (2018). Chapter 4: Mesh, In: *Midas GTS NX User Manual*, (pp. 145-146).
- Möller, S.C. and Vermeer, P.A. (2008). "On numerical simulation of tunnel installation", *Tunnelling and Underground Space Technology*, 23(4), 461-475, <https://doi.org/10.1016/j.tust.2007.08.004>.
- Mousivand, M. and Maleki, M. (2018). "Constitutive models anddetermining methods effects on application of convergence-confinement method in underground excavation", *Geotechnical and Geological Engineering*, 36(3), 1707-1722, <https://doi.org/10.1007/s10706-017-0426-2>.
- Ng, C.W.W., Sun, H.S., Lei, G.H., Shi, J.W. and Mašin, D. (2015). "Ability of three different soil constitutive models to predict a tunnel's response to basement excavation", *Canadian Geotechnical Journal*, 52(11), 1685-1698, <https://doi.org/10.1139/cgj-2014-0361>.
- Oettl, G., Stark, R.F. and Hofstetter, G. (1998). "A comparison of elastic-plastic soil models for 2D FE analyses of tunnelling", *Computers and Geotechnics*, 23(1-2), 19-38, [https://doi.org/10.1016/S0266-352X\(98\)00015-9](https://doi.org/10.1016/S0266-352X(98)00015-9).
- Rocdata Software Manual. (2004). *R.I.R. Version 3.0 User's Guide of RocData: Strength analysis of rock and soil masses using the generalized Hoek-Brown, Mohr-Coulomb, Barton-Bandis and power curve failure critera*, Toronto, Ontario, Canada, (n.d.).
- Rukhaiyar, S. and Samadhiya, N.K. (2016). "Analysis of tunnel considering Modified Mohr-Coulomb criteria", *Recent Advances in Rock Engineering (RARE 2016)*, Atlantis Press.
- Sarikhani Khorami, M. (2012). "Analysis of geomechanical parameters and in situ stress of rock mass in Isfahan-Shiraz railway tunnel using back analysis based on displacement monitoring", M.Sc. Thesis, Isfahan University of Technology, Isfahan, Iran.
- Sharifzadeh, M., Daraei, R. and Broojerdi, M.S. (2012). "Design of sequential excavation tunneling in weak rocks through findings obtained from displacements based back analysis", *Tunnelling and Underground Space Technology*, 28, 10-17, <https://doi.org/10.1016/j.tust.2011.08.003>.
- Singh, B. and Goel, R.K. (1999). *Rock mass classification: A practical approach in civil engineering*, (Vol. 46), Elsevier.
- Su, K., Zhang, Y.-J., Chang, Z.-H., Wu, H.-G., Wang, T. and Zhou, W. (2019). "Transverse extent of numerical model for deep buried tunnel excavation", *Tunnelling and Underground Space Technology*, 84, 373-380, <https://doi.org/10.1016/j.tust.2018.11.034>.
- Sulem, J., Panet, M. and Guenot, A. (1987). "Closure analysis in deep tunnels", *International Journal of Rock Mechanics and Mining Sciences and Geomechanics Abstracts*, 24(3), 145-154, [https://doi.org/10.1016/0148-9062\(87\)90522-5](https://doi.org/10.1016/0148-9062(87)90522-5).
- Sun, H., Liu, S., Zhong, R. and Du, L. (2020). "Cross-section deformation analysis and visualization of shield tunnel based on mobile

- tunnel monitoring system", *Sensors*, 20(4), 1006, <https://doi.org/10.3390/s20041006>.
- Vakili, K., Lavasan, A.A., Schanz, T. and Datcheva, M. (2014). "The influence of the soil constitutive model on the numerical assessment of mechanized tunneling", *Proceedings of the 8th European Conference on Numerical Methods in Geotechnical Engineering*, Delft, The Netherlands, 889-894.
- Vitali, O.P.M., Celestino, T.B. and Bobet, A. (2018). "3D finite element modelling optimization for deep tunnels with material nonlinearity", *Underground Space*, 3(2), 125-139, <https://doi.org/10.1016/j.undsp.2017.11.002>.
- Xing, Y., Kulatilake, P. and Sandbak, L.A. (2018). "Investigation of rock mass stability around the tunnels in an underground mine in USA using three-dimensional numerical modeling", *Rock Mechanics and Rock Engineering*, 51(2), 579-597, <https://doi.org/10.1007/s00603-017-1336-6>.
- Xue, Y., Zhou, B., Li, S., Qiu, D., Zhang, K., and Gong, H. (2021). "Deformation rule and mechanical characteristic analysis of subsea tunnel crossing weathered trough", *Tunnelling and Underground Space Technology*, 114, 103989, <https://doi.org/10.1016/j.tust.2021.103989>.
- Yasitli, N.E. (2016). "Comparison of input parameters regarding rock mass in analytical solution and numerical modelling", *Journal of African Earth Sciences*, 124, 497-504, <https://doi.org/10.1016/j.jafrearsci.2016.08.010>.
- Zhao, C., Alimardani Lavasan, A., Barciaga, T., Kämper, C., Mark, P. and Schanz, T. (2017). "Prediction of tunnel lining forces and deformations using analytical and numerical solutions", *Tunnelling and Underground Space Technology*, 64, 164-176, <https://doi.org/10.1016/j.tust.2017.01.015>.

This article is an open-access article distributed under the terms and conditions of the Creative Commons Attribution (CC-BY) license.

